



A LETTERS JOURNAL EXPLORING
THE FRONTIERS OF PHYSICS

OFFPRINT

**Permutation complexity of spatiotemporal
dynamics**

J. M. AMIGÓ, S. ZAMBRANO and M. A. F. SANJUÁN

EPL, **90** (2010) 10007

Please visit the new website
www.epljournal.org

TARGET YOUR RESEARCH WITH EPL



Sign up to receive the free EPL table of contents alert.

www.epljournal.org/alerts

Permutation complexity of spatiotemporal dynamics

J. M. AMIGÓ¹, S. ZAMBRANO² and M. A. F. SANJUÁN²

¹ *Centro de Investigación Operativa, Universidad Miguel Hernández - 03202 Elche, Spain, EU*

² *Departamento de Física, Universidad Rey Juan Carlos - Tulipán s/n 28933 Madrid, Spain, EU*

received 19 January 2010; accepted in final form 23 March 2010

published online 29 April 2010

PACS 05.45.Jn – High-dimensional chaos

PACS 05.45.Tp – Time series analysis

PACS 87.19.1e – EEG and MEG

Abstract – We call permutation complexity the kind of dynamical complexity captured by any quantity or functional based on order relations, like ordinal patterns and permutation entropies. These mathematical tools have found interesting applications in time series analysis and abstract dynamical systems. In this letter we propose to extend the study of permutation complexity to spatiotemporal systems, by applying some of its tools to a time series obtained by coarse-graining the dynamics and to state vectors at fixed times, considering the latter as sequences. We show that this approach allows to quantify the complexity and to classify different types of dynamics in cellular automata and in coupled map lattices. Furthermore, we show that our analysis can be used to discriminate between different types of spatiotemporal dynamics registered in magnetoencephalograms.

Copyright © EPLA, 2010

Introduction. – Permutation entropy was introduced in [1] as a complexity measure for time series. Roughly speaking, permutation entropy replaces the probabilities of length- L symbol blocks in the definition of Shannon's entropy by the probabilities of length- L *ordinal patterns* — a digest of the ups and downs of L consecutive elements of a time series. Permutation entropy was later extended, both in metric and topological versions, to one-dimensional dynamical systems in ref. [2], and to higher-dimensional systems in refs. [3,4]. Since then, different techniques based on the analysis of ordinal patterns, that we refer to as *permutation complexity analysis*, have found a number of interesting applications: Estimation of metric and topological entropy [4,5], complexity analysis of time series [6], detection of determinism in noisy time series [7,8], recovery of control parameters in symbolic sequences of unimodal maps [9] and characterization of synchronization [10]. In all these applications, computational simplicity and robustness against observational noise have been a crucial advantage.

In this letter we propose to extend the study of permutation complexity to spatiotemporal systems. We apply our ideas to two well-known models of spatiotemporal dynamics, cellular automata (CA) and coupled map lattices (CML), as well as to the experimental spatiotemporal data provided by magnetoencephalograms (MEGs). Our analysis is divided into two (complementary) parts. The first part is an analysis of a time series obtained by

coarse-graining the dynamics considered. The second part is an analysis of the state vector at fixed times. We show that the first part provides an estimation of the dynamical complexity, and its combination with the second one provides further insights, especially when it comes to the classification of different types of dynamical behavior. Considering this, and similarly to recent works where tools of network analysis were used for time series analysis [11,12], our work reveals a link between the analysis of spatially extended systems and novel ideas from time series analysis.

Models of spatiotemporal systems. – The analysis that we propose can be applied to spatiotemporal data of the form $\{\mathbf{x}_t\}_{t=1}^T = \{\mathbf{x}_1, \mathbf{x}_2, \dots, \mathbf{x}_T\}$, where $\mathbf{x}_t = (x_t(1), x_t(2), \dots, x_t(N))$ is the state vector at time t of a system of N sites, each component $x_t(i)$ being the state of the i -th site at time t . The numerical data that we consider in this letter are generated with one-dimensional CA and CMLs featuring a next-neighbor local rule of evolution,

$$x_{t+1}(i) = f(x_t(i-1), x_t(i), x_t(i+1)), \quad (1)$$

and the periodic boundary condition $x_t(1) = x_t(N+1)$.

Some tools of permutation complexity. – The basic tools that we use in our analysis are the following. Consider for simplicity that $\{z_n\}_{n=1}^M = \{z_1, z_2, \dots, z_M\}$ is a sequence of real numbers. We say that a length- L block

(word, window, ...) $\{z_j\}_{j=n}^{n+L-1} = \{z_n, z_{n+1}, \dots, z_{n+L-1}\}$ defines the *ordinal pattern* $\pi = \langle \pi_0, \dots, \pi_{L-1} \rangle$ of length L if

$$z_{n+\pi_0} < z_{n+\pi_1} < \dots < z_{n+\pi_{L-1}}, \quad (2)$$

where in case $z_i = z_j$ and $i < j$, we set $z_i < z_j$ for definiteness. Alternatively we say that $\{z_n\}_{n=1}^M$ is of type π . Note that π_0, \dots, π_{L-1} is a *permutation* of the numbers $0, 1, \dots, L-1$. We denote by \mathcal{S}_L the set of ordinal patterns of length L —or ordinal L -patterns.

Given $\{z_n\}_{n=1}^M$ we can compute $N(L)$, the number of ordinal patterns of length L found in the sequence. For an i.i.d sequence and $L! \ll M$, we expect $N(L) \approx L!$. If $z_{n+1} = f(z_n)$ with f a piecewise monotone map (*e.g.*, the logistic or tent map), then there is an L such that $N(L) < L!$, *i.e.*, there exist *forbidden ordinal patterns* [7]. Furthermore, if $L! \ll M$, the topological entropy of f , $h_{top}(f)$, can be estimated by the *topological permutation entropy* of order L , $h_{top}^*(L) = \frac{1}{L} \log N(L)$ [2], since

$$\lim_{L \rightarrow \infty} h_{top}^*(L) \equiv \lim_{L \rightarrow \infty} \frac{1}{L} \log N(L) = h_{top}(f). \quad (3)$$

Thus, a simple method to quantify the complexity of a sequence consists in counting $N(L)$ [7].

Another tool is related to the detection of determinism in noisy time series $\{z_n\}_{n=1}^M$ [8]. In this case, one can perform a chi-square test of independence of the sequence with the *null hypothesis*

$$H_0: \text{the } z_n \text{ are white noise.}$$

Let K be the number of non-overlapping sliding windows of size L , $\{z_n\}_j^{j+L-1}$, in the series $\{z_n\}_{n=1}^M$, $1 \leq j \leq M-L+1$, with $L \ll M$. Let ν_π be the number of visible windows of type $\pi \in \mathcal{S}_L$. Then the parameter (or “statistic”)

$$\chi^2(L) = \frac{L!}{K} \sum_{\pi \in \mathcal{S}_L: \text{visible}} \nu_\pi^2 - K \quad (4)$$

provides a way to accept or reject the null hypothesis with a significance level $1 - \alpha$: Accept if $\chi^2 < \chi_{L!-1, 1-\alpha}^2$, reject if $\chi^2 > \chi_{L!-1, 1-\alpha}^2$, where $\chi_{L!-1, 1-\alpha}^2$ is the upper $1 - \alpha$ critical point for the chi-square distribution with $L! - 1$ degrees of freedom. For this test, it is recommended to use values of L such that $5L! \lesssim K$ (see [8] for details). The parameter $\chi^2(L)$ acts as a quantifier of the complexity of the sequence: The closer the sequence is to an i.i.d. sequence, the more similar the values of the ν_π are for all $\pi \in \mathcal{S}_L$, which leads to lower values of $\chi^2(L)$.

There are, of course, other more sophisticated tools, but we show below that these modest ones are already useful to quantify the dynamical complexity of spatially extended systems.

Permutation complexity analysis of spatiotemporal dynamics. — We describe now the two types of analysis that we apply to spatiotemporal data $\{\mathbf{x}_t\}_{t=1}^T$. The first one, which we call *temporal* analysis, applies to a symbolic sequence obtained via discretization of

the spatiotemporal dynamics. We consider here binary sequences $\{\mathbf{s}_t\}_{t=1}^T$, where $\mathbf{s}_t = (s_t(1), s_t(2), \dots, s_t(N))$,

$$s_t(i) = \begin{cases} 0, & \text{if } x_t(i) < x_c(i), \\ 1, & \text{if } x_t(i) > x_c(i), \end{cases} \quad (5)$$

and $x_c(i)$ is a given threshold for the site i . With this symbolic sequence we can build a univariate time series $\{\phi_t\}_{t=1}^T = \{\phi_1, \phi_2, \dots, \phi_T\}$, where

$$\phi_t = \phi(\mathbf{s}_t) = \sum_{i=1}^N \frac{s_t(i)}{2^i} \in [0, 1]. \quad (6)$$

The *temporal* analysis is performed by either counting the number of ordinal L -patterns $N(L)$ in $\{\phi_t\}_{t=1}^T$ (using, in general, overlapping sliding windows) or by calculating the parameter $\chi^2(L)$ for $\{\phi_t\}_{t=1}^T$, for different values of L . We call $\chi_{time}^2(L)$ the result.

We propose as well a *spatial* analysis that consists in calculating $\chi^2(L)$ for the state vector \mathbf{x}_t , viewed as a sequence $\{x_t(j)\}_{j=1}^N$, for different fixed times t . Then average over t and set $\langle \chi^2(L) \rangle = \chi_{space}^2(L)$. We call $\chi_{time}^2(L)$ and $\chi_{space}^2(L)$ *regularity parameters*.

Application to CA. — As a first example of application of permutation complexity analysis to spatiotemporal systems we consider one-dimensional elementary CA. This means that \mathbf{x}_t is a string of 0s and 1s, of finite length N in simulations; hence, $f(p, q, r) \in \{0, 1\}$, where f is the local rule of evolution, and $p, q, r \in \{0, 1\}$. Since the states of CA are already discrete, we set $\mathbf{s}_t = \mathbf{x}_t$ in eq. (6) to obtain $\{\phi_t\}_{t=1}^T$. Note that the local rule f of any CA induces a selfmap F of the whole configuration space, called the *global transition map*.

First consider the CA with $f(p, q, r) = p + r \pmod 2$, which is an instance of a positively expansive CA, thus with complicated dynamics. A space-time diagram of this system is shown in fig. 1(a). The topological entropy for this CA is $h_{top}(F) = 2 \log 2 = 2$ bit/iteration [13].

We can compute $N(L)$ for $\{\phi_t\}_{t=1}^T$. If $L! \ll T$, we can as well define the topological permutation entropy of the CA as $h_{top}^*(L) = \log(N(L))/L$, and similarly to eq. (3), it can be proved that $\lim_{L \rightarrow \infty} h_{top}^*(L) = h_{top}(F)$, the topological entropy of the CA. This is numerically confirmed in fig. 1(b), where we can observe $h_{top}^*(L) = \log(N(L))/L$ converging to the value 2 (bit/iteration) as L increases.

The above tools of permutation complexity can also be used for the classification of CA. The 256 possible elementary CA were extensively studied in a series of papers by Chua and collaborators; see, *e.g.*, [14]. Wolfram proposed to classify them [15,16] according to their asymptotic behavior as:

Class W1: The configurations converge to a fixed point as, *e.g.*, $f(p, q, r) = \frac{1}{2}[1 + \text{sign}(2p + 4q + 2r - 5)]$.

Class W2: Time evolution yields a sequence of simple stable or periodic structures as, *e.g.*, $f(p, q, r) = p$.

Class W3: The behavior is “chaotic” as, *e.g.*, $f(p, q, r) = p + q + r + qr \pmod 2$.

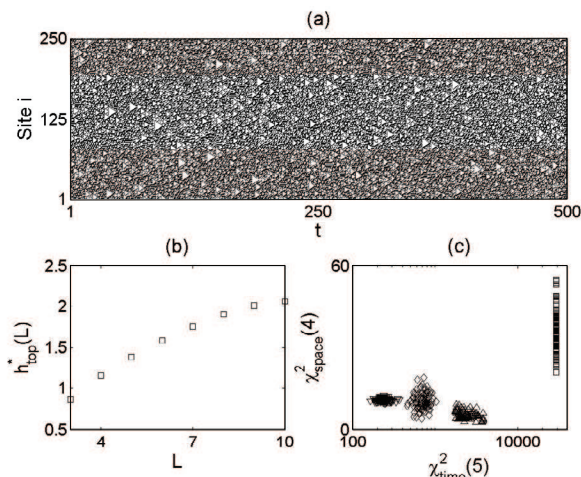


Fig. 1: (a) Space-time plot of a trajectory of the expansive CA with local rule $f(p, q, r) = p + r \bmod 2$ and $N = 250$ (white dots are 0, black dots are 1). (b) Computation of $h_{top}^*(L)$ for different L values (\square). A convergence to the expected value of 2 bits/iteration is observed. (c) $\chi_{time}^2(5)$ vs. $\chi_{space}^2(4)$ for 100 different random initial conditions of *Class W1* (\square), *Class W2* (\diamond), *Class W3* (∇) and *Class W4* (\triangle).

Class W4: Time evolution yields a regular spatiotemporal pattern with localized structures that move around and interact in very complicated ways as, e.g., $f(p, q, r) = (1 + p)qr + q + r \bmod 2$.

Here we are dealing with CA of finite length $N = 250$ and thus with $2^{250} \approx 1.8 \cdot 10^{75}$ possible states, which imposes an upper bound in their period (2^{250} iterations). However, we analyze them in much shorter time scales, so the classification above makes full sense. To our knowledge there is no quantitative way to distinguish these four complexity classes. With this scope in mind, we have calculated the regularity parameters for each of the instances provided above. Let us point out that $\chi_{space}^2(L)$ has to be modified from the form of eq. (4), because \mathbf{x}_t is now a binary sequence. For a sequence of two symbols, 0 and 1, the χ^2 for windows of size L is

$$\chi^2(L) = \frac{(2^L \nu_0 - L - 1)^2}{2^L(L+1)} + \left(1 - \frac{L+1}{2^L}\right) (2^L \nu_1 - 1)^2$$

with ν_0 the number of times the pattern $\pi_0 = \langle 0, 1, 2, \dots, L-1 \rangle$ has been observed, and ν_1 is the number of patterns of length L such that $\pi \neq \pi_0$.

To avoid too small samples in our numerical simulations with $N = 250$, we take $L \leq 4$ for $\chi_{space}^2(L)$ (so as $L! \ll N$). For $\chi_{time}^2(L)$ we may choose L larger. In fig. 1(c) we plot the values of $\chi_{time}^2(5)$ against those of $\chi_{space}^2(4)$ for 100 different realizations of each of the representatives given above; they clearly cluster in different, non-overlapping regions. It is also interesting to notice that the lower values of $\chi_{time}^2(5)$ are obtained for the *Class W3* CA, which displays spatiotemporal chaotic behaviour. We have repeated the same calculations with a few more

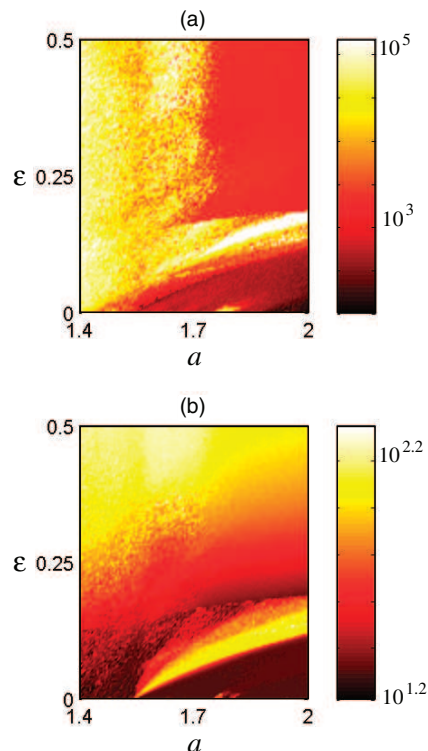


Fig. 2: (Colour on-line) Colormap of (a) $\chi_{time}^2(5)$ and (b) $\chi_{space}^2(4)$. The first test allows to identify the region of spatiotemporal chaos (dark/red region), whereas the second one gives important information about the spatial regularity of the system for ε and a . Both parameters combined can distinguish between different phases of the CML.

representatives, with similar results, showing that our regularity parameters capture the basic features of the different complexity classes of CA.

Application to CMLs. – A similar analysis can be applied to CMLs, introduced by Kaneko [17,18] as a simple test bed for spatiotemporal chaos. We consider here CMLs of the type

$$x_{t+1}(i) = (1 - \varepsilon)g(x_t(i)) + \frac{\varepsilon}{2} [g(x_t(i-1)) + g(x_t(i+1))] \quad (7)$$

which correspond to *diffusive* CMLs with coupling constant $\varepsilon > 0$. In our simulations, $0 \leq \varepsilon \leq 0.5$ and g is the map [21]

$$g(x) = 1 - ax^2, \quad x \in [-1, 1]. \quad (8)$$

For the calculation of $\chi_{time}^2(L)$ in CMLs, the discretization of the data is done using eq. (5) with $x_c(i) = 0$. This discretization has been shown to capture most of the important features of the CML dynamics [19,20].

The results of our analysis are shown in fig. 2. In fig. 2(a) we can observe $\chi_{time}^2(5)$. Remarkably, there are clearly two zones of dark/light colors (red-yellow), and the dark one (low $\chi_{time}^2(5)$ values) corresponds to the zone of

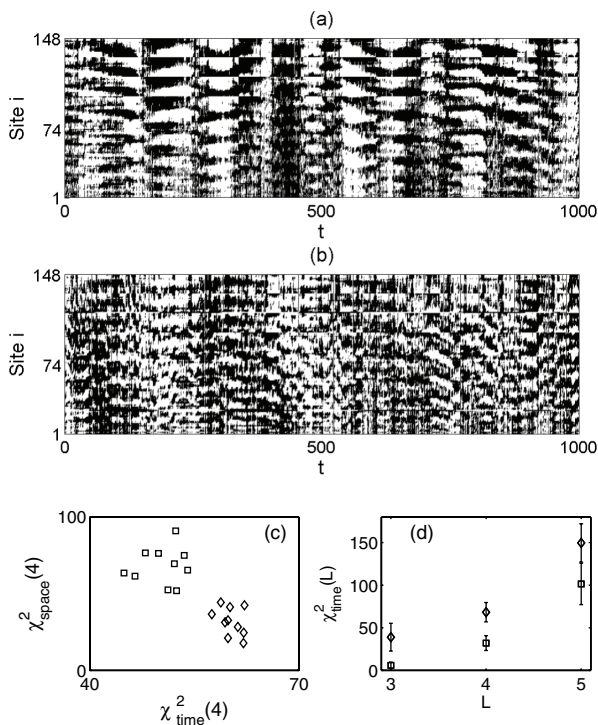


Fig. 3: Space-time plot of discretized MEGs (white dots are 0, black dots are 1) from (a) control patient and (b) patient with ADHD. (c) $\chi_{time}^2(4)$ vs. $\chi_{space}^2(4)$ for 10 different data samples from control patient (\square) and patient with ADHD (\diamond). They cluster in non-overlapping regions, so this plot clearly discriminates these two types of data. (d) Computation of $\chi_{time}^2(L)$ for three L values for the control patient (\square) and patient with ADHD (\diamond), error bars are statistical errors.

spatiotemporal chaos sketched by Kaneko in [21]. Thus, $\chi_{time}^2(5)$ can be used to quantify the complexity of the global temporal evolution of the system. A similar result is obtained with $N(L)$, $L \geq 5$. In fact, simulations show that these two simple measures behave similarly to the largest Lyapunov exponent. Recall that this is analogous to the results obtained in CA, where low values of $\chi_{time}^2(L)$ were obtained for the chaotic CA. Thus, again, a permutation complexity analysis of $\{\phi_t\}_{t=1}^T$ provides a simple way to measure the dynamical complexity of a CML.

We can also compute $\chi_{space}^2(L)$, as shown for $L=4$ in fig. 2(b). It provides a clear picture of the dependence of the spatial regularity of the system on ε and a , which is nontrivial although it typically increases with ε . This is not surprising, since for larger ε values we expect to see an increasing correlation between the dynamics of neighbouring sites, which implies that the spatial regularity increases. Finally, we point out that simulations performed with instances of the six major ‘‘phases’’ [21] observed in CMLs, show that they can be classified combining $\chi_{time}^2(L)$ and $\chi_{space}^2(L)$.

Application to MEGs. – As a final example of application of our analysis we consider data sets of MEGs

from two patients, a control patient and a patient with attention-deficit/hyperactivity disorder (ADHD). MEGs were acquired for both patients in the same conditions with a 148-channel whole-head magnetometer (MAGNES 2500 WH, 4D Neuroimaging, San Diego, California). Each data set consists of 148 noisy time series comprising 1000 measurements per channel, which amounts to a set of spatiotemporal data $\{\mathbf{x}_t\}_{t=1}^T$ with $N=148$ and $T=1000$. A total of 10 such series were recorded from each patient. Here we do not know anything about the topology of the network that connects the sites, although channel i is close to either channel $i-1$, channel $i+1$ or both (see [22] for a detailed description). To obtain $\{\phi_t\}_{t=1}^T$ we use again eq. (6), but now the discretization of eq. (5) is done with the threshold $x_c(i) = \langle x_t(i) \rangle$, *i.e.*, the time average of the time series of the considered channel. A space-time plot of $\{\mathbf{s}_t\}_{t=1}^{1000}$ for one data set of the control patient is shown in fig. 3(a), and in fig. 3(b) for the patient with ADHD.

We have performed a permutation complexity analysis of the 10 data sets of both patients. In fig. 3(c) we show $\chi_{time}^2(4)$ against $\chi_{space}^2(4)$ for each data set. Clearly they cluster in non-overlapping regions. The value of $\chi_{time}^2(L)$ is enough to discriminate between data of the patients, as shown in fig. 3(d). In fact, we observe for the control patient lower values of $\chi_{time}^2(L)$, which suggests that the spatiotemporal dynamics registered in its MEGs is more complex than for the patient with ADHD. This agrees with results obtained with other complexity measures [22]. Our analysis, though, reveals that χ_{space}^2 is smaller for the patient with ADHD. Similar results were obtained when testing our techniques with data sets of different control and ADHD patients. We believe that this information might be helpful for the analysis of this type of data in diagnosis. Finally, we want to point out that the MEGs data are quite noisy, so we think that these results show that our analysis is quite robust against observational noise, a quality that was observed in previous applications of permutation complexity analysis [7,8].

Conclusions. – We have shown that the concepts and tools of permutation complexity provide a simple approach to the study and classification of the dynamical complexity of spatiotemporal systems. We believe that the computational simplicity and robustness against observational noise of this approach makes it particularly advantageous for the study of large data sets.

We thank Dr A. FERNÁNDEZ from Centro de Magnetoencefalografía at Universidad Complutense de Madrid for kindly providing us the MEG data. Financial support from the Ministry of Education and Science (Spain) under Project No. FIS2006-08525, and from the Ministry of Science and Innovation (Spain) under Projects No. MTM2009-11820 and No. FIS2009-09898 is acknowledged.

REFERENCES

- [1] BANDT C. and POMPE B., *Phys. Rev. Lett.*, **88** (2002) 174102.
- [2] BANDT C., KELLER G. and POMPE B., *Nonlinearity*, **15** (2002) 1595.
- [3] AMIGÓ J. M., KENNEL M. B. and KOCAREV L., *Physica D*, **210** (2005) 77.
- [4] AMIGÓ J. M. and KENNEL M. B., *Physica D*, **231** (2007) 137.
- [5] AMIGÓ J. M., KOCAREV L. and TOMOVSKI I., *Physica D*, **228** (2007) 77.
- [6] CAO Y., TUNG W., GAO J. B., PROTOPODESCU V. A. and HIVELEY L. M., *Phys. Rev. E*, **70** (2004) 046217.
- [7] AMIGÓ J. M., ZAMBRANO S. and SANJUÁN M. A. F., *EPL*, **79** (2007) 50001.
- [8] AMIGÓ J. M., ZAMBRANO S. and SANJUÁN M. A. F., *EPL*, **83** (2008) 60005.
- [9] ARROYO D., ALVAREZ G. and AMIGÓ J. M., *Chaos*, **19** (2009) 023125.
- [10] MONETTI R., BUNK W., ASCHENBRENNER T. and JAMITZKY F., *Phys. Rev. E*, **79** (2009) 046207.
- [11] ZHANG J. and SMALL M., *Phys. Rev. Lett.*, **96** (2006) 238701.
- [12] XU X., ZHANG J. and SMALL M., *Proc. Natl. Acad. Sci. U.S.A.*, **105** (2008) 19601.
- [13] D'AMICO M., MANZINI G. and MARGARA L., *Theor. Comput. Sci.*, **290** (2003) 1629.
- [14] CHUA L. O., SBITNEV V. I. and YOON S., *Int. J. Bifurcat. Chaos Appl. Sci. Eng.*, **15** (2005) 1045.
- [15] WOLFRAM S., *A New Kind of Science* (Wolfram Media, Champaign) 2002.
- [16] WOLFRAM S., *Physica D*, **10** (1984) 1.
- [17] KANEKO K., *Prog. Theor. Phys.*, **69** (1983) 1427.
- [18] KANEKO K., *Prog. Theor. Phys.*, **69** (1984) 480.
- [19] PETHEL S. D., CORRON N. J. and BOLLT E., *Phys. Rev. Lett.*, **96** (2006) 034105.
- [20] PETHEL S. D., CORRON N. J. and BOLLT E., *Phys. Rev. Lett.*, **99** (2007) 214101.
- [21] KANEKO K., *Physica D*, **34** (1989) 1.
- [22] FERNÁNDEZ A., QUINTERO J., HORNERO R., ZULUAGA P., NAVAS M., GÓMEZ C., ESCUDERO J., GARCÍA-CAMPOS N., BIEDERMAN J. and ORTIZ T., *Biol. Psychiatry*, **65** (2009) 571.